

# INTERNATIONAL SOCIETY FOR SOIL MECHANICS AND GEOTECHNICAL ENGINEERING



*This paper was downloaded from the Online Library of the International Society for Soil Mechanics and Geotechnical Engineering (ISSMGE). The library is available here:*

<https://www.issmge.org/publications/online-library>

*This is an open-access database that archives thousands of papers published under the Auspices of the ISSMGE and maintained by the Innovation and Development Committee of ISSMGE.*

*The paper was published in the proceedings of the 20<sup>th</sup> International Conference on Soil Mechanics and Geotechnical Engineering and was edited by Mizanur Rahman and Mark Jaksa. The conference was held from May 1<sup>st</sup> to May 5<sup>th</sup> 2022 in Sydney, Australia.*

## Large shearing device – influence of swing suspension on direct simple shear device

Appareil de cisaillement de grande taille - influence du mouvement crée par le chariot sur l'appareil de cisaillement simple direct

**Elin Bergliv, Qi Jia & Jan Laue**

*Luleå University of Technology, Luleå, Sweden*

**Tommy Edeskär**

*Geoskills AB, Luleå, Sweden*

**ABSTRACT:** A large direct simple shear device has been developed to test aggregates up to 200 mm nominal size. The simple shear apparatus is based on a novel design using a swing suspension. The sample is contained in a steel wire reinforced rubber membrane fixed at the top to the load frame and at the bottom to a mobile swing. The shearing is conducted by moving a hanging swing horizontally in a load frame by a hydraulic actuator. Another actuator is applying vertical stress on the top of the sample. The swing suspension causes the shear swing to lift and the horizontal actuator to tilt during the shearing procedure. This can cause deviations for the shear stress and shear displacement. The effect of the swing suspension movement on the results has been investigated for 20 tests performed.

A geometrical relation was defined between the uplift of the shear swing and the tilt of the actuator. The shear displacement and shear stress can be calculated either considering or ignoring the uplift and tilt. Comparing the two different ways of evaluating, the results show that there is a minor difference between considering and ignoring swing suspension. The difference in results is in the range of the measurement accuracy of the actuator. The shear displacement deviation was found to be completely geometrically dependent on the horizontal displacement of the swing. This effect can easily be predicted and considered during the evaluation of the test result.

**RÉSUMÉ :** Un dispositif de cisaillement simple direct grand format a été développé pour tester des matériaux granulaires d'un diamètre maximum de 200 mm. L'appareil de cisaillement simple est d'une conception nouvelle utilisant un chariot pivotant. L'échantillon est contenu dans une membrane en caoutchouc renforcée de fil d'acier fixée au sommet du bâti de chargement et à la base du chariot mobile. Le cisaillement est effectué en déplaçant le chariot suspendu horizontalement dans le bâti de chargement avec une presse hydraulique, qui peut également contrôler la contrainte horizontale. Une autre presse applique une contrainte verticale sur le dessus de l'échantillon. L'oscillation cause un soulèvement de l'appareil de cisaillement et provoque l'inclinaison de la presse horizontale pendant la procédure de cisaillement. Cela peut entraîner une déviation de la contrainte de cisaillement et la déformation de cisaillement.

L'effet du mouvement oscillant sur les résultats a été étudié pour 20 tests. Une relation géométrique a été définie entre le soulèvement dû à l'oscillation et l'inclinaison de la presse. La déformation de cisaillement et la contrainte de cisaillement peuvent être calculées en considérant ou en ignorant le soulèvement et l'inclinaison. Comparant ces deux manières différentes d'évaluation, les résultats montrent que la différence est mineure. La différence entre les résultats se situe dans la plage de précision de la presse. L'écart de déplacement de cisaillement s'est avéré être complètement dépendant géométriquement du déplacement horizontal de la presse. Cet effet peut être facilement prédit et pris en compte lors de l'évaluation du résultat du test.

**KEYWORDS:** Direct simple shear; granular material; design of laboratory equipment

### 1 INTRODUCTION

Testing of large sized rock and soil materials is challenging since it requires large sized samples and large forces. There is a variety of different findings in the literature on the dependence of grain size on strength and deformation properties of large grained materials, here defined as material having maximum grain size over 100 mm. For large sized granular materials no dependence in size has been reported by Fumagalli (1969), Matsuoka & Liu (1998), and Hu et al (2011). Lower strength for larger grains is reported by Marsal (1967), Marachi et al (1972), and Ovalle et al (2014). Most studies find that confining stress (or normal stress), initial void ratio and grain crushing are more important factors for strength and deformation properties, compared to initial maximum grain size.

At Luleå University of Technology the first large sized direct simple shear device was developed in the early 2000's. The size

of the sample was 640 mm in diameter and 400-600 mm in height, and the maximum grain size tested was up to 150 mm (Berglund & Forsman, 2008; Silfvernagel, 2009). In a master's thesis (Berglund & Forsman, 2008) some future improvements were suggested, including increased rigidity in the bottom and top of the sample to ensure horizontal shearing. The membrane was attached to the top stamp using tie down straps. For large shearing displacements, high stresses, and the tilting of the top stamp, the membrane sometimes slipped in the top fastening. Of practical concern was to keep the membrane attached to the top and bottom stamp at large shear displacements and stresses.

The new large shearing device was developed to be able to perform direct simple shear tests more safely than with the preceding shear device. In a first stage the size was increased, which also requires larger forces and shearing displacements. The design was completely reworked to deal with the drawbacks of the previous device. The swing suspension was chosen instead

of pre-stressing the device to allow large forces.

## 2 THE LARGE SHEARING DEVICE

Figure 1 shows a sketch of the novel large shearing device. The outer extension of the device is the free-standing load frame, about 4 m high. In the top of the load frame the vertical actuator is attached. The other end of the actuator is attached to the top part, which distributes the force on the sample. Four guides, made from smooth, low-friction steel, keeps the top part in place. The guides are pair-wise attached to beams in the load frame. The fit between the guides and the holes in the top part is tight and it makes the top part move only up and down as controlled by the vertical actuator and not move sideways or tilt. As the top part only can move up or down, and not tilt, the vertical force is evenly distributed on the sample.

A steel wire lined rubber membrane is bolted to the mount ring on the shear swing. On top of the membrane another mount ring is attached. The membrane is attached to the mount rings with bolts through a fringe, which is reinforced with a steel ring of thickness 20 mm. The mount rings are present to avoid sliding of the ends of the sample. The height of the mount rings is 200 mm. The sample material is placed in the membrane in layers and compacted.

The shear swing is connected to the load frame with four rods, one in each corner of the swing. The rods are suspended in the top of the load frame. One side of the shear swing is connected to the horizontal actuator. The horizontal actuator is connected to the load frame via protruding beams.

The vertical force and displacement are measured in the vertical actuator. Analogously, the horizontal force and displacement are measured in the horizontal actuator. Two string potentiometers placed on the sides of the membrane measure the length of the membrane. Another string potentiometer measure the circumference change in the middle of the membrane. The pore pressure is measured in the top and bottom of the sample using pore pressure cells. Load cells attached to the four rods measure force in each rod.

The shear test is usually performed by pulling the shear swing with the horizontal actuator in one direction, see Figure 2, but two-directional loading is also possible. The shearing is conducted to exceed the shear strain 0.15 radians. If no failure is apparent in the  $\tau$ - $\sigma$ -plot, the failure is defined at the shear strain 0.15 rad according to Swedish standards (SIS, 1991).

## 3 MATERIALS AND METHOD

### 3.1 Testing setup

20 tests have been performed with varying sample materials and stress levels. The sample materials included a uniformly graded sand with grain size 0-2 mm, a well-graded large grained material with grain size 0-200 mm, and a naturally rounded, gap-graded material with grain size 0-100 mm. The normal stresses used were in the range 80-492 kPa. Two different sample sizes, 500 mm and 1000 mm membrane height have been used. For all tests the membrane diameter was 1000 mm, which made the slenderness of the samples different. See Table 1 for testing configurations.

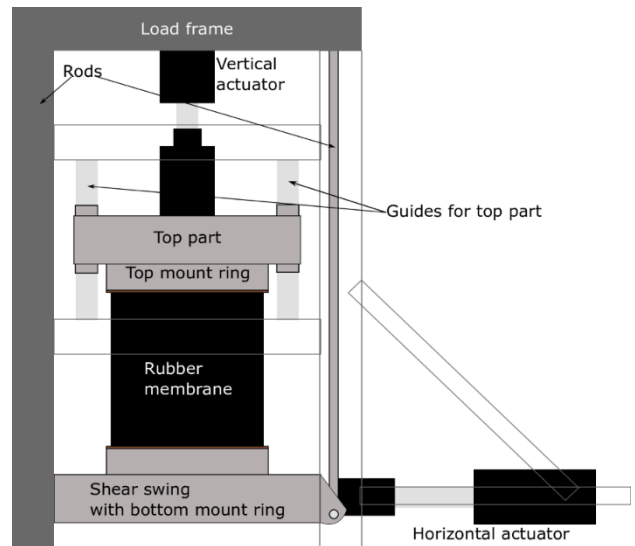


Figure 1. Sketch of the large shearing device. Not in scale. Some parts of the load frame are made see-through to show details (right side of the Figure).

The shear swing was suspended in the four rods. During shearing, in addition to the horizontal displacement, the fixed length of the rods caused the swing to lift slightly, see Figure 2. This caused the horizontal load cell to tilt slightly, see Figure 3. The measured force in the horizontal load cell consists of a horizontal and vertical component. The horizontal component is the shear force  $T$  and the monitored horizontal force is denoted using  $H$ . Further the monitored horizontal stroke  $h$  could deviate from the shear displacement  $x$ .

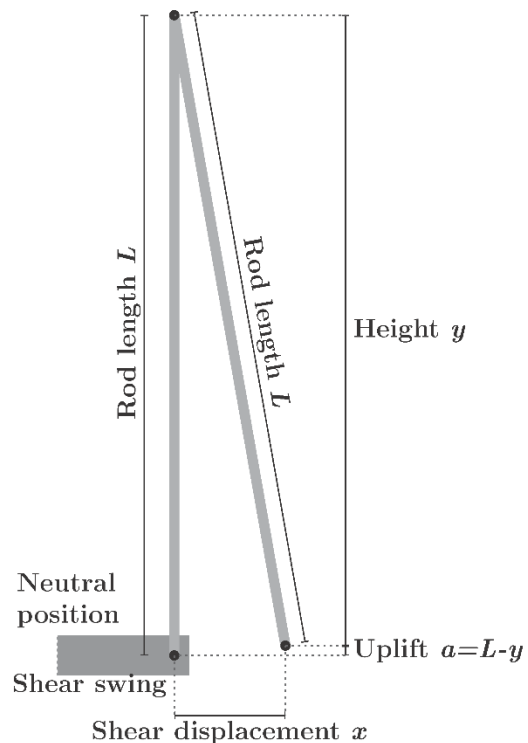


Figure 2. The uplift of the shear swing.

Table 1: Test configuration and sample material description

Test number	Grain size (mm)	Material type	Normal stress (kPa)	Sample height (mm)
Test01	0-2	Crushed, uniformly graded	80	1000
Test02	0-2	Crushed, uniformly graded	160	1000
Test03	0-2	Crushed, uniformly graded	320	1000
Test04	0-200	Crushed, well-graded	80	1000
Test05	0-2	Crushed, uniformly graded	75	500
Test06	0-2	Crushed, uniformly graded	150	500
Test07	0-100	Rounded grains, gap graded	492	500
Test08	0-100	Rounded grains, gap graded	199	500
Test09	0-95	Rounded grains, gap graded	344	500
Test10	0-95	Rounded grains, gap graded	198	500
Test11	0-200	Crushed, well-graded	83	500
Test 12	0-200	Crushed, well-graded	164	500
Test13	0-200	Crushed, well-graded	161	500
Test14	0-200	Crushed, well-graded	323	500
Test15	0-200	Crushed, well-graded	163	500
Test16	0-200	Crushed, well-graded	163	500
Test17	0-200	Crushed, well-graded	163	500
Test18	0-200	Crushed, well-graded	162	500
Test19	0-200	Crushed, well-graded	163	500
Test20	0-200	Crushed, well-graded	319	500

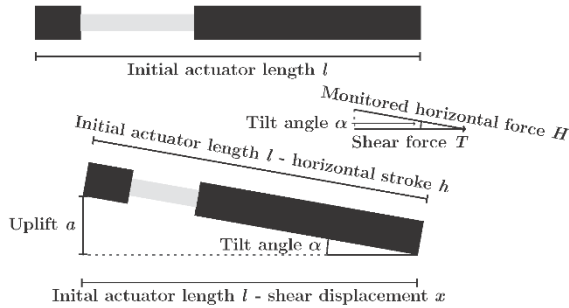


Figure 3. The actuator tilts for large shear displacements.

### 3.2 Method

In the following part the method for the geometrical analysis is introduced. First the geometrical components are denoted, see Figure 4. Below there is a list of all the notations.

- $\alpha$  - Tilt angle [rad or °]
- $a$  - Uplift [mm]
- $h$  - Monitored horizontal stroke [mm]
- $l$  - Initial actuator length [mm]
- $x$  - Shear displacement [mm]
- $H$  - Monitored horizontal force [kN]
- $L$  - Rod length [mm]
- $T$  - Shear force [kN]

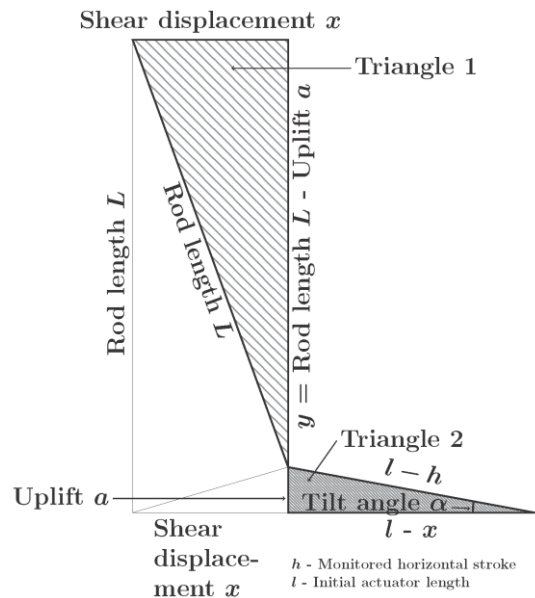


Figure 4. Notations for calculations and connection between actuator tilt and shear swing uplift.

The uplift of the shear swing causes the horizontal actuator to tilt. The relationship of the uplift  $a$  as a function of horizontal stroke  $h$  is derived in Eq.1 – Eq.3.

Pythagoras's theorem on triangle 1 (see Figure 4).

$$L^2 = x^2 + y^2 \quad (1a)$$

$$L^2 = x^2 + (L - a)^2 \quad (1b)$$

$$L^2 = x^2 + L^2 - 2aL + a^2 \quad (1c)$$

$$0 = x^2 - 2aL + a^2 \quad (1d)$$

$$x = \pm\sqrt{2aL - a^2} \quad (1e)$$

The next step is to express uplift  $a$  as a function of horizontal stroke  $h$  from triangle 2 using Pythagoras's theorem (see Figure 4).

$$a^2 + (l - x)^2 = (l - h)^2 \quad (2a)$$

$$a^2 + l^2 - 2lx + x^2 = l^2 - 2lh + h^2 \quad (2b)$$

$$a^2 - 2lx + x^2 = h^2 - 2lh \quad (2c)$$

Substituting the expression for  $x$  from Eq. 1e into Eq. 2c gives Eq. 3.

$$a^2 - 2l\sqrt{2al - a^2} + 2aL - a^2 = h^2 - 2lh \quad (3a)$$

$$2aL - 2l\sqrt{2al - a^2} - h^2 + 2lh = 0 \quad (3b)$$

The rod length  $L$  is 3178 mm. As the shear swing is in its initial, neutral position, before the shearing phase starts, the initial length of the horizontal actuator,  $l$ , is noted.

Solving Eq. 3b for uplift  $a$  with the monitored values of horizontal stroke  $h$  was the next step in the calculation. The solution was done using Python's SymPy.solve module (Meurer et al, 2017). Eq. 3b has two roots, but any roots outside the range  $0 \leq a \leq 100$  was considered implausible.

This solution is strictly geometrical, only dependent of the length of the actuator,  $l$ , for each test. After finding the uplift  $a$ , Eq. 1e was used to calculate the shear displacement  $x$ .

The tilt angle  $\alpha$  was calculated with Eq. 4.

$$\sin \alpha = \frac{a}{l-h} \quad (4)$$

The tilt angle  $\alpha$  was used to find the shear force  $T$ , with Eq. 5.

$$T = H \cos \alpha \quad (5)$$

The monitored horizontal stroke  $h$  was compared with its horizontal component, the shear displacement  $x$ . The monitored shear force  $H$  was compared with its horizontal component, the shear force  $T$ . The difference was compared with respect to the accuracy level of the measuring system. The accuracy was 0.001 mm for the displacement measurement and 1 N for the force measurements. If the difference was less than the accuracy, the difference would be within the error margin of the setup. Errors within the error margin are neglected.

#### 4 RESULTS

The uplift  $a$  as a function of horizontal stroke  $h$  for the performed tests is presented in Figure 5. All the tests show a similar uplift pattern with increasing horizontal stroke  $h$  and the range is narrow.

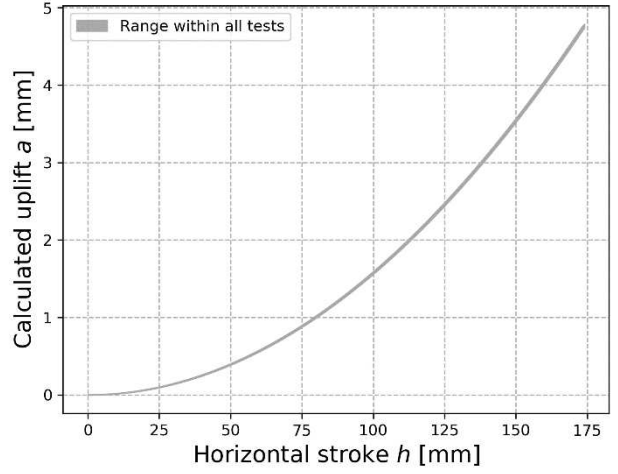


Figure 5. The uplift plotted against the horizontal stroke for all tests.

Using Eq. 1e, the shear displacement  $x$  was found. Shear displacement  $x$  is plotted against the horizontal stroke  $h$  in Figure 6. In the figure it is impossible to discern any difference between the variables. To evaluate the difference between the variables, the difference of the shear displacement  $x$  to the horizontal stroke  $h$  is plotted against the horizontal stroke in Figure 7. The accuracy of the measuring system, 0.001 mm for distance, is added in the figure. The difference increases as the horizontal stroke increases, with a value of 110-115 mm horizontal stroke as the value where the difference is measurable. The first four tests are performed with 1000 mm height membrane, requiring a shear displacement of 150 mm to exceed the target shear strain 0.15 rad. The following 16 tests are performed with 500 mm height membrane, only requiring 75 mm shear displacement to exceed 0.15 rad shear strain.

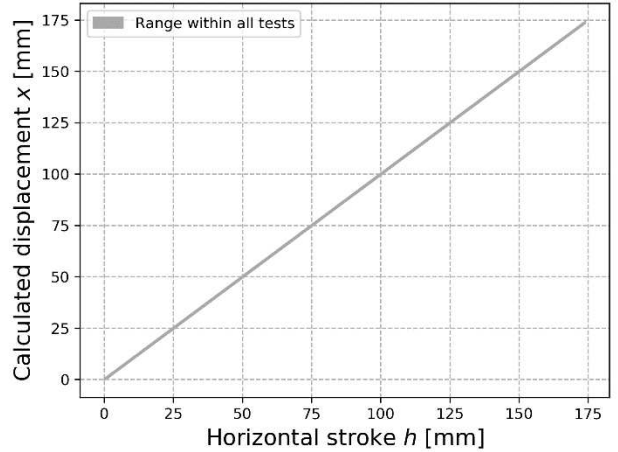


Figure 6. Shear displacement  $x$  versus horizontal stroke  $h$ .

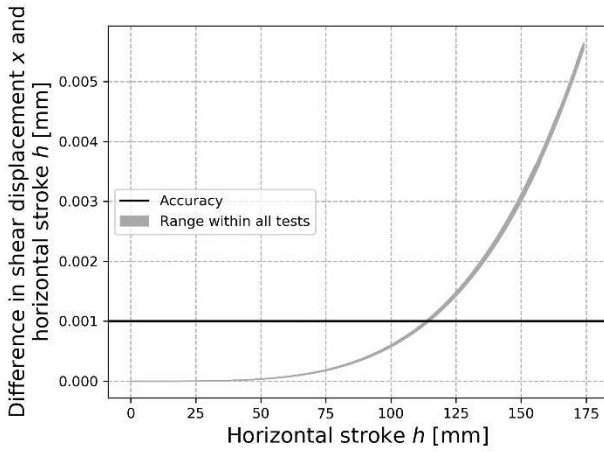


Figure 7. The difference in the shear displacement  $x$  and horizontal stroke  $h$  plotted against horizontal stroke  $h$ . The measurement accuracy is highlighted in the figure, as the horizontal line.

The tilt angle  $\alpha$  was found from the uplift using Eq. 4. After determining the tilt angle  $\alpha$ , it is possible to find the horizontal component of the monitored shear force, using Eq. 5. The difference between the shear force  $T$  and monitored horizontal force  $H$  is plotted against horizontal stroke  $h$  in Figure 8. The accuracy of the measuring system for force is 1 N and this level is also plotted in the figure. All the tests show difference below the accuracy limit and the difference can therefore be neglected. For force and stress the swing suspension does not have influence on the results in this test series.

The difference between the shear force  $T$  and the monitored horizontal force  $H$  is further termed “force difference”. The force difference depends on the horizontal stroke  $h$ , where the force difference increases for increasing horizontal stroke  $h$ . This is a result of that the uplift  $a$ , and thus also the tilt angle  $\alpha$ , increases for increased horizontal stroke  $h$ . The force difference is also dependent on the normal stress. The force difference increases by increasing normal stress, see Figure 9.

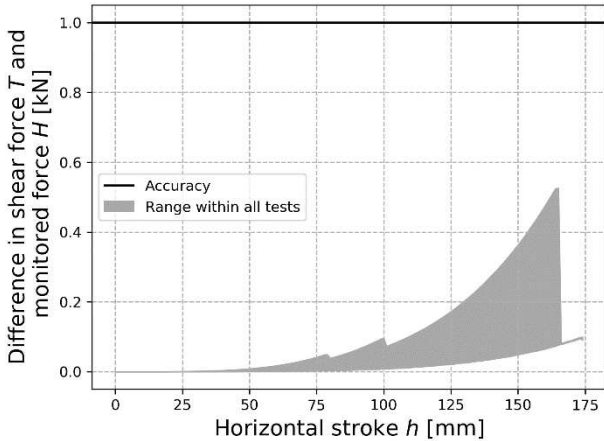


Figure 8. Difference between the shear force  $T$  and monitored horizontal force  $H$  against horizontal stroke  $h$ . The measurement accuracy is highlighted in the figure, as the horizontal line.

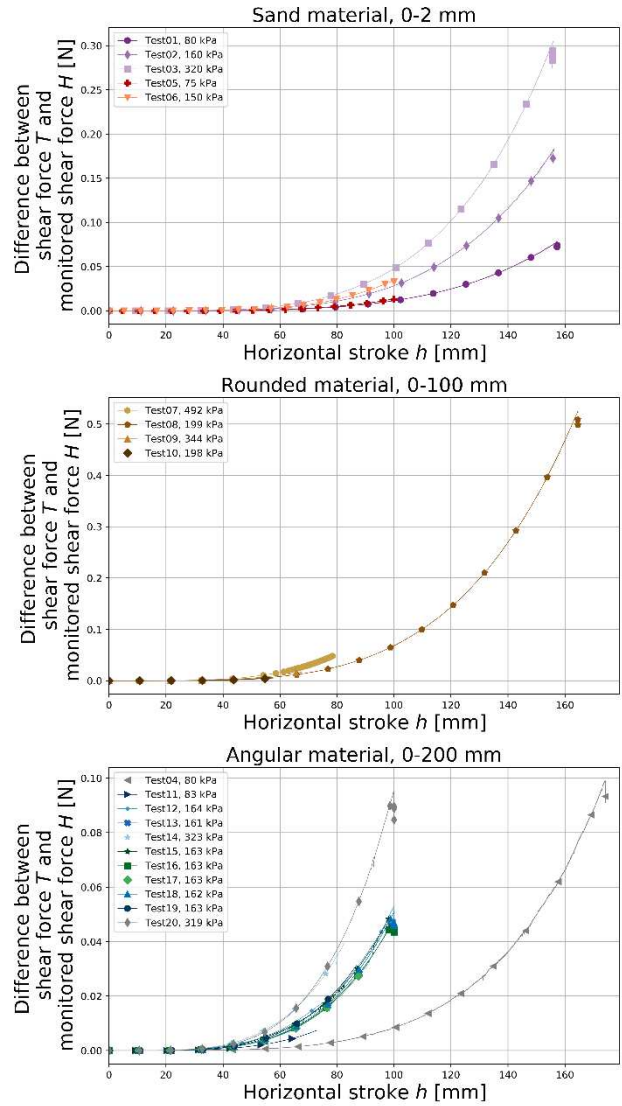


Figure 9. The force difference presented by material type. The influence of the horizontal stroke  $h$  and the normal stress is apparent.

The following assumptions were made in the setup of the analysis. The vertical actuator was assumed to have no inclination at the start of each test. The rods were also assumed to hang fully vertically with no inclination to the vertical plane. The starting position of the shear swing for the shearing phase is termed the neutral position. This is defined as the position where the horizontal force is very close to zero at the start of the saturation phase, and this position is kept constant until the shearing phase. Horizontal forces can accumulate during saturation and consolidation phases, and some small changes to the horizontal position might occur. The neutral position might also vary slightly from test to test depending on the installation procedure of a single test. The neutral position is defined in terms of length of the horizontal actuator at the start of the shearing phase. The maximum initial length of the horizontal actuator was 2214 mm, and the shortest length was 2176 mm. The difference was 38 mm, and no consideration was taken to the possible influence of the different neutral positions.

## 5 CONCLUSION

The influence of the vertical dislocation during the shearing of the sample is small. Up to 110 mm total horizontal displacement the effect is within the accuracy of measurements.

For all tests the target shear strain was 0.15 rad. The needed shear displacement to achieve the target shear strain varies with sample height. In this test series, the sample height 500 mm required a shear displacement of 75 mm. This shear displacement gave no influence from the swing suspension. For the larger sample height 1000 mm the target shear displacement was 150 mm, which gave influence from the swing suspension.

The influence from the swing suspension on horizontal displacement is easily corrected by using the calculated shear displacement  $x$  for further calculations and analysis instead of the monitored horizontal stroke  $h$ .

In the case of the horizontal forces, the difference is less than the error margin of the system and can therefore be neglected. The influencing factors, horizontal displacement and normal stress, might increase in future testing and this analysis is vital to exclude swing suspension influence on horizontal forces.

## 6 ACKNOWLEDGEMENTS

This research was partially funded by the Swedish joint research program for road and railway geotechnology BIG (Branschsamverkan I Grunden). Thanks to Thomas Forsberg of the Mining and Civil Engineering Lab at Luleå University of Technology.

## 7 REFERENCES

- Berglund, A. & Forsman, J. 2008. *Grovkorniga jordars mekaniska egenskaper - laborietester med storskalig skjvapparat* Luleå University of Technology, Luleå. Master's thesis. [In Swedish].
- Fumagalli, E. 1969. Tests on Cohesionless Materials for Rockfill Dams. *Journal of the Soil Mechanics and Foundations Division* 95, 313-332.
- Hu, W.; Dano, C.; Hicher, P.-Y.; Le Touzo, J.-Y.; Derkx, F. & Merliot, E. 2011. Effect of Sample Size on the Behavior of Granular Materials. *Geotechnical Testing Journal, ASTM International*, 34, 186-197.
- Marachi, N. D.; Chan, C. K. & Seed, H. B. 1972. Evaluation of Properties of Rockfill Materials. *Journal of the Soil Mechanics and Foundation Division* 98, 95-114.
- Marsal, R. J. 1967. Large Scale Testing of Rockfill Materials. *Journal of the Soil Mechanics and Foundations Division* 93, 27-43.
- Matsuoka, H. & Liu, S. 1998. Simplified direct box shear test on granular materials and its application to rockfill materials. *Soils and Foundations* 38, 275-284.
- Meurer, A.; Smith, C. P.; Paprocki, M.; Čertík, O.; Kirpichev, S. B.; Rocklin, M.; Kumar, A.; Ivanov, S.; Moore, J. K.; Singh, S.; Rathnayake, T.; Vig, S.; Granger, B. E.; Muller, R. P.; Bonazzi, F.; Gupta, H.; Vats, S.; Johansson, F.; Pedregosa, F.; Curry, M. J.; Terrel, A. R.; Roučka, Š.; Saboo, A.; Fernando, I.; Kulal, S.; Cimrman, R. & Scopatz, A. SymPy: symbolic computing in Python. *PeerJ Computer Science* 3:e103
- Ovalle, C.; Frossard, E.; Dano, C.; Hu, W.; Maiolino, S. & Hicher, P.-Y. 2014. The effect of size on the strength of coarse rock aggregates and large rockfill samples through experimental data. *Acta Mechanica, Springer Nature* 225, 2199-2216
- Silfvernagel, H. 2009. *Storskaliga skjv försök på grovkornig jord*. Luleå University of Technology. Master's thesis. [In Swedish]
- SIS. 1991. *Geotechnical tests – Shear strength – Direct simple shear test, CU- and CD-tests – Cohesive soil*. SIS – Standardiseringskommisionen i Sverige. SS 027127.